Asian Journal of Chemistry; Vol. 27, No. 10 (2015), 3625-3632

ASIAN JOURNAL OF CHEMISTRY

http://dx.doi.org/10.14233/ajchem.2015.18889

Preparation and Physico-Chemical Characterization of Modified Acidic and Basic Metal Oxide Catalysts

E.H. EL-MOSSALAMY[1], M. EL-BATOUTI[2,*], T. AHMED[3], L.M. AL-HARBI[3], N.F. AL HARBY[4] and A.A. AL-OWAIS[5]

[1]Chemistry Department, Faculty of Science, Benha University, Benha, Egypt
[2]Chemistry Department, Faculty of Science, Alexandria University, Alexandria, Egypt
[3]Chemistry Department, Faculty of Science, King Abdulaziz University, 21589 Jeddah, P.O. Box 80203, Saudi Arabia
[4]Chemistry Department, Faculty of Science and Arts, Al Qassim University, Buraydah 52571, Saudi Arabia
[5]Chemistry Department, King Saud University, P.O. Box 272047, Riyadh-11352, Saudi Arabia

*Corresponding author: E-mail: mervette_b@yahoo.com

Received: 1 December 2014; *Accepted*: 20 February 2015; *Published online*: 22 June 2015; AJC-17315

The effect of the type of precursor used in the preparation of pure and modified aluminium oxide (Al_2O_3, as an acidic oxide) and magnesium oxide (MgO, as a basic oxide) on their structural and surface properties were studied and characterized using different physico-chemical techniques. Thermal analyses (including thermogravimetry, differential thermal analysis) and X-ray diffraction analysis were performed to analyze all the oxide catalyst samples under investigation. In addition, measurements of the acidity and basicity of all samples were performed *via* the temperature programmed desorption of basic or acidic probe molecules (pyridine and formic acid, respectively) using the thermogravimetric analysis technique.

Keywords: Alumina, Thermal analyses, Temperature programmed desorption, Magnesia.

INTRODUCTION

Investigation of the effect of different variables on the activity and selectivity of a catalyst are essential in order to identify the optimum conditions that permit the maximum efficiency of specified catalyst for a specific reaction[1,2]. Over the past few years, a better understanding of the co-functioning of catalysts and their supports has been achieved. The difference between the promoter and the catalyst was described to be a difference in quantity, *i.e.* if the support exceeds the quantity of the catalyst it becomes a support otherwise it is a promoter[3].

Alumina is commonly used for the different species of aluminium oxides which exists in at least five thermodynamically stable phases and many meta-stable transition forms[4]. It has a wide variety of applications, *e.g.* as an adsorbent, support and as a catalyst. Transitional alumina formed *via* thermal decomposition of the hydroxides constitutes the largest group among the materials used as adsorbents. The loss of hydroxyl groups results in structure defects in the alumina and oxygen lattice. Alumina is an amphoteric substance that can act as an acid in a basic medium or a base in acidic medium. One of the most striking properties of alumina is the transition phases that exist over a large temperature range[3]. The catalytic properties of alumina have already been focused on a number of studies that concerning with the synthesis of different chemical compounds[5,6]. This is due to the fact that alumina has remarkable adsorbent properties and its capability of activating a certain bonds, *e.g.* H-H bonds, C-H bonds and C-C bonds. Because of this fact, it is very active in exchange reactions[7,8], double bond isomerization of alkenes or skeletal isomerization of alkenes[9,10], cracking of hydrocarbons and dehydration of alcohols to ethers or alkenes[11-20]. Magnesia has been given a considerable attention as a catalyst. It is used in many catalyzed reactions, *e.g.* decomposition of alcohols[21], synthesis of α, β unsaturated nitriles from ketone and methanol[22], the aldol addition of acetone and the hydrogenation of conjugated dienes[23]. Like any catalyst, the surface properties of magnesia are greatly dependent on its preparation conditions[24]. Magnesia powder with a large surface area (S_{BET} = 350 m^2 g^{-1}) with higher solid basicity has been obtained by microwave cold plasma heating[25].

Characterization of the acid/base properties of magnesia has been carried out using different probe molecules like nitrous oxide[26], pyridine[27] and carbon dioxide[28]. The amount and strength of basic sites have been found to be enhanced by the modification of magnesia with suitable amounts of different ions[26], *e.g.* Na^+, Al^{3+} and Zr^{4+}. The main factors generating

stronger basicity were mentioned to be fewer Mg atoms coordinated to the central oxygen atom in the basic site and more oxygen atoms coordinated to the Mg atoms adjacent to the central oxygen atoms[29]. It has been found that when the calculated amount of the basic sites of MgO and CaO, prepared from $Mg(OH)_2$ and $Ca(OH)_2$, is plotted against the calcination temperature, the basicity increases at 400 °C and reaches its maximum between 500-600 °C then it decreases above 700 °C[30,31].

The preparation parameters are known to play vital role in determining the surface structure and characteristics of a solid catalyst. In the present investigation, the catalysts used (alumina and magnesia) were prepared by two different methods, namely, precipitation and calcination of the pure catalysts. The parent materials were thermally characterized by TG and DTA techniques to get useful information about the temperature range at which these parent materials start to decompose and finally form stable products of known structures. The parent materials were thermally treated at different calcination temperatures and characterized by X-ray diffraction analysis (XRD). The acid/base properties of these catalysts were measured using pyridine and/or formic acid as probe molecules. Finally, a correlation between the preparation conditions and modification of these catalysts was performed.

EXPERIMENTAL

Preparation of pure and modified oxides: Pure alumina catalysts were prepared by two different methods:

(a) Precipitation: Aluminium hydroxide was precipitated by the drop wise addition of ammonium hydroxide, with continuous stirring, to a hot solution of $AlCl_3$ (BDH, England). The resulting precipitate was then washed several times using distilled water. Drying was carried out for 24 h at 120 °C. The dried sample was subjected to calcination at different temperatures (*i.e.* 500, 600, 700, 800 and 900 °C), in air, for 5 h in a muffle furnace. These alumina samples are denoted as AlO-P.

(b) Calcination: In this method, the alumina was prepared by direct calcination of $Al(NO_3)_2{\cdot}9H_2O$ (BDH, England) at the same temperatures given above and at the same conditions. These samples are denoted as AlO-C.

As described above, two pure magnesium oxide samples were prepared by two different methods:

(a) Precipitation: Magnesium oxide was prepared by the drop wise addition of ammonium hydroxide, with continuous stirring, to a hot solution of $MgCl_2{\cdot}6H_2O$ (BDH, England). The hydroxide produced was then washed several times with distilled water, dried in an oven for 24 h at 120 °C and then it was calcined at 500, 600, 700, 800 and 900 °C, in air, for 5 h in a muffle furnace. These samples are denoted as Mg-P.

(b) Calcination: The second MgO sample was prepared by direct calcination of $MgCO_3$ (BDH, England), in air, at the same temperatures given above and at the same conditions. These samples are denoted as Mg-C.

Modified samples of pure Al_2O_3 and MgO calcined at 600 °C were obtained by the addition of 5 wt. % of either Na_2O or P_2O_5 (BDH, England).

Thermogravimetric analysis: Thermogravimetric analysis (TGA) and differential thermal analysis (DTA) were carried out utilizing a Thermal Analyst 2000 TA instrument (U.S.A.) controlling a 2050 thermogravimetric analyzer. A platinum ceramic sample boat was used for TGA analysis. Samples weighing 10.0 mg were heated up to 900 °C at 5 °C min^{-1}, in a flow (40 mL/min) of nitrogen (N_2) atmosphere.

X-ray diffraction analysis: XRD patterns were obtained using a Philips 1840 diffractometer at RT. Diffraction patterns were obtained with Ni-filtered CuK_α radiation ($\lambda = 0.154056$ nm). The patterns obtained were matched with the standard data[32,33] for the purpose of phase identification.

Acidity and basicity measurements: The acidity and basicity of some selected catalysts were determined thermogravimetrically by the adsorption and desorption method using pyridine and formic acid as probe molecules, respectively. 200 mg of each sample was pre-heated in an oven at 250 °C for 2 h and was then kept in a desiccator together with a beaker containing pyridine or formic acid at ambient temperature for 2 weeks prior to analysis. 15 mg of each sample, after exposure to pyridine or formic acid, was subjected to TG analysis in the temperature range between ambient to 230 °C (at a heating rate of 20 °C/min) in dry N_2 (40 mL/min). The acidity or the basicity was calculated as mg pyridine or formic acid/g catalyst.

RESULTS AND DISCUSSION

Pure and modified alumina: The two alumina precursors, [*i.e.* $Al(NO_3)_2{\cdot}9H_2O$ and $Al(OH)_3{\cdot}xH_2O$] and their calcination products were characterized using different techniques such as TGA, DTA, XRD and TPD of adsorbed pyridine.

Thermogravemtric analysis (TGA and DTA): Table-1 represents the TG and DTA data of the two alumina precursors, [*i.e.* $Al(NO_3)_3{\cdot}9H_2O$ and $Al(OH)_3{\cdot}xH_2O$]. The TG data of $Al(NO_3)_3{\cdot}9H_2O$ between ambient temperature and up to 500 °C exhibits three weight loss steps. The first step appeared between 72-85 °C and is accompanied by 7.2 % weight loss. This step could be attributed to partial dehydration of the parent salt. The second, strong, step between 95-170 °C was accompanied by 57.8 % weight loss. It is ascribed to the combination of dehydration and decomposition processes. The third and final step extended between 180-500 °C. It is accompanied by a weight loss of 18.5 %. It could be attributed to the subsequent dehydroxylation processes. The total weight loss at 500 °C is about 83.5 %, which is in a good agreement with theoretical expectation (about 86.4 %) for Al_2O_3 formation. This result may indicate that up to 500 °C the product Al_2O_3 is still containing some strongly attached surface hydroxyl groups. The corresponding DTA data of $Al(NO_3)_3{\cdot}9H_2O$ shows that the endothermic effects corresponding to the first two weight loss steps are composite in nature and are maximized at 72, 85 and 136 °C, respectively. There is no thermal response attributed to the third weight loss step (about between 200-500 °C). The TGA data of $Al(OH)_3{\cdot}xH_2O$ reveals three weight loss steps between ambient temperature and 500 °C. The first step is rather slow and gradual. It takes place between 31-220 °C and is accompanied by 13.42 % weight loss. This is followed by the second sharp step between 220-295 °C with 47.43 % weight loss. Finally, the third step (between 295-500 °C) is accompanied by a weight loss of 6.44 %. This brings the total weight loss, on heating to 500 °C, to 67.39 % of the original sample weight. These weight loss steps are attributed to the

TABLE-1
THERMOGRAVEMTRIC (TGA) AND DIFFERENTIAL THERMOGRAVEMETRIC (DTA) ANALYSIS DATA FOR THE NON ISOTHERMAL DECOMPOSITION OF $Al(NO_3)_3{\cdot}9H_2O$ AND $Al(OH)_3$

Sample	TGA data			DTA data T_{max}	ΔE (kJ/mol)
	Decomposition steps	Temperature ranges (°C)	Mass loss (%)		
$Al(NO_3)_3{\cdot}9H_2O$	1	72-85	7.20	85 °C	49.0
	2	95-170	57.80	136 °C	41.0
	3	180-500	18.50		
$Al(OH)_3$	1	31-220	13.42		
	2	220-295	47.43	265 °C	47.0
	3	295-500	6.44		

dehydration processes. Theoretically, the transformation of $Al(OH)_3$ to Al_2O_3 should result in a total weight loss of 34.6 %. This difference is due to the existence of water of hydration. The corresponding DTA data shows relevant endothermic peak at 265 °C. The activation energies, ΔE (kJ/mol), for the decomposition steps of both samples ($Al(NO_3)_3{\cdot}9H_2O$ and $Al(OH)_3$) are given in Table-1.

X-ray diffraction analysis (XRD): Fig. 1 exhibits the X-ray diffractograms of $Al(NO_3)_3{\cdot}9H_2O$ calcined at 700, 800 and 900 °C (denoted as, AlO-C). Samples calcined at 500 and 600 °C were poorly crystalline. The sample calcined at 700 °C shows a weak pattern of γ-alumina. Further calcination at 800 °C has given a well developed γ-alumina pattern. Sample calcined at 900 °C, however, shows α-alumina as being the major phase besides the γ-alumina as a minor one. The XRD patterns of the precipitated alumina (denoted as, AlO-P) are shown in Fig. 2. It is obvious that γ-alumina is gradually developed with increasing the calcination temperature from 500 to 900 °C. A minor α-alumina phase begins to be detectable only for the sample calcined at the 900 °C.

Acidity measurements (temperature programmed desorption): The number of acid sites on alumina surface was found to increase by anions modification and decrease by cations modification. Figs. 3 and 4 shows the temperature programmed desorption curves of the adsorbed pyridine on different alumina samples, namely AlO-C and AlO-P, respectively. It is obvious from Fig. 3 that the acidity of the AlO-C system decreases as the calcination temperature increase from 500 to 600 °C; this can be attributed to the low crystallinity of the calcined sample at 600 °C. The acidity then increases for the sample calcined

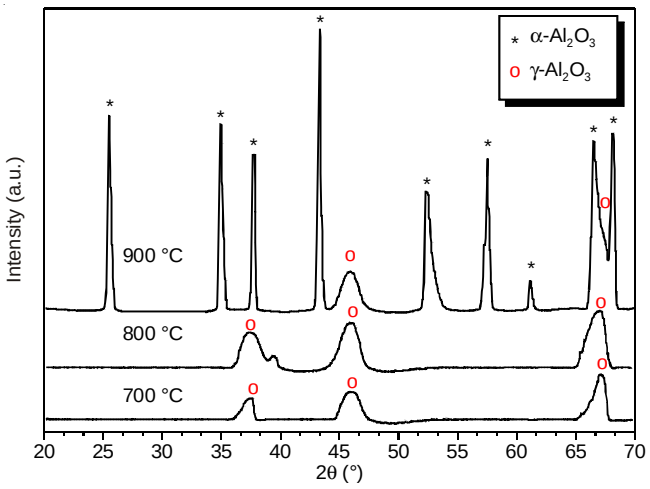

Fig. 1. XRD patterns of AlO-C catalysts calcined at different temperatures

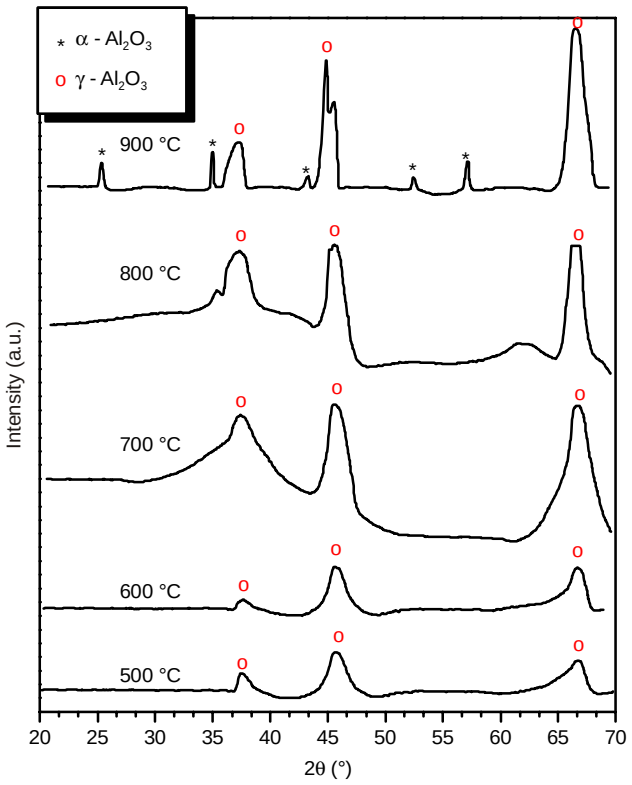

Fig. 2. XRD patterns of AlO-P catalysts calcined at different temperatures

at 700 °C which may be due to the enhancement of crystallinity and the appearance of the γ-alumina phase as revealed by the XRD results. Owing to the amorphous nature of γ-alumina which has a defect structure with layers of O^{2-} ions in a cubic close packed arrangement and layers of Al^{3+} ions some having tetrahedral and some having octahedral coordination in the oxygen lattice, one can attribute the increase in acidity of the 700 °C calcined sample to the appearance of a new Lewis acid sites accompanying the appearance of the γ-alumina phase. Finally, the acidity decreases again for samples calcined at 800 and 900 °C. This can be due to the expected decrease in surface area at higher calcination temperatures and, also to the appearance of the α-alumina phase for the sample calcined at 900 °C. The acidity measured for the AlO-P system is shown in Fig. 4. It shows a gradual decrease in acidity as the calcination temperature increases from 500 to 900 °C. This behaviour could be explained on the assumption that calcination of $Al(OH)_3$ at 500 °C produces a microporous Al_2O_3. Calcination above 500 °C and up to 900 °C is expected to result in a gradual decrease in surface area and increases the extent of dehydroxylation. This may account for the decrease in acidity

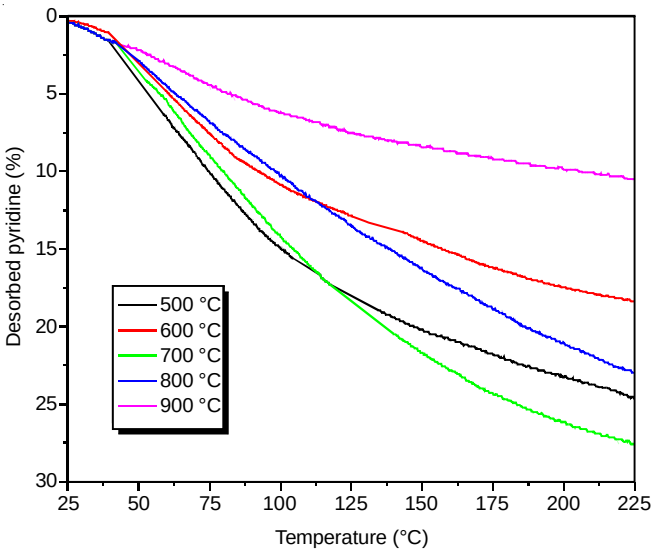

Fig. 3. Temperature programmed desorption (TPD) curves of the adsorbed pyridine over AlO-C catalysts calcined at different temperatures

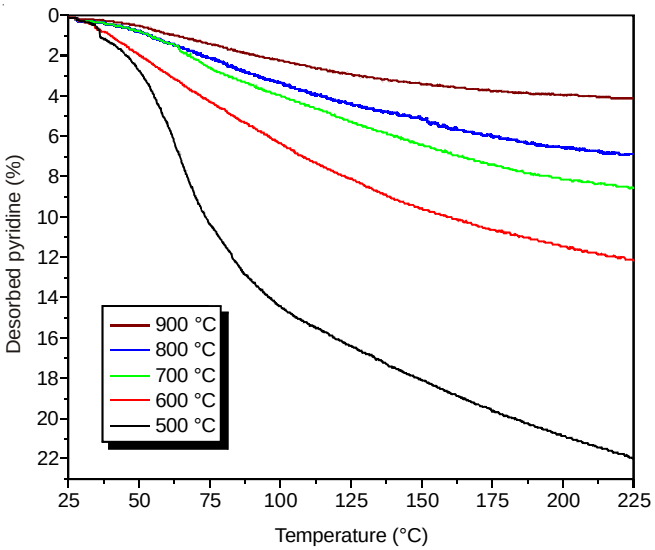

Fig. 4. Temperature programmed desorption (TPD) curves of the adsorbed pyridine over AlO-P catalysts calcined at different temperatures

as the calcination temperature increases. Close inspection of the temperature programmed desorption curves of both alumina samples (Figs. 3 and 4) may help us to draw the following points:

Alumina samples prepared by calcination of aluminium nitrate have shown higher acidity compared to those prepared from the precipitated aluminium hydroxide. This is clearly displayed in Fig. 5 where the amounts of pyridine desorbed from AlO-C samples were always higher than the corresponding amount desorbed from AlO-P at all calcination temperatures.

Pyridine is desorbed through two steps; the first step at < 100 °C is fast while the second is a gradual step and extended from 100 to 225 °C.

Increasing the calcination temperature has resulted in a decrease in the total amount of pyridine desorbed at 225 °C. It also affects the nature of the two desorption steps, where at lower calcination temperature the two desorption steps are well separated.

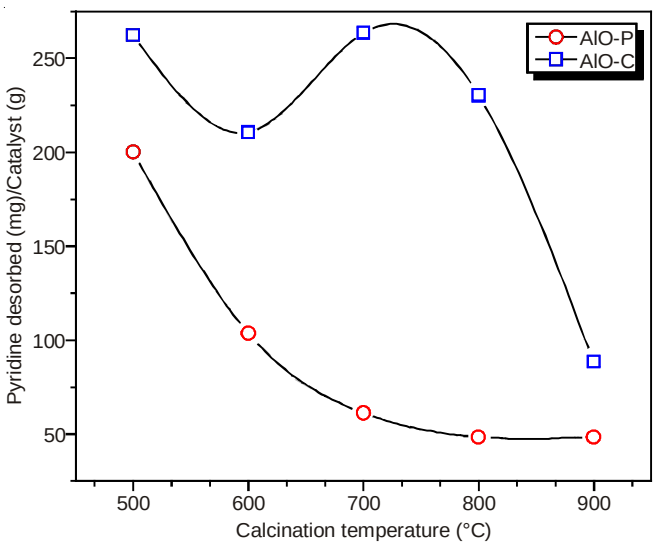

Fig. 5. Acidity of pure alumina catalysts (C and P) calcined at different temperatures

From the above points we can conclude the following:

Pyridine is adsorbed on the alumina surface through two adsorption types namely; H-Py and L-Py. The hydrogen bonded pyridine H-Py is desorbed at < 100 °C. Accordingly, this type is strongly dependent on the population of surface hydroxyls. This may explain the dependence of the first step on calcination temperature, where the concentration of hydroxyl groups decreased markedly with increasing the calcination temperature.

Alumina shows Lewis type acidity (L-Py). This may account for the second desorption step at > 100 °C. The gradual desorption of L-Py (till 225 °C) shows that there are different types of Lewis adsorbed pyridine. In fact, γ-alumina shows two types of Al^{3+} ions in the crystal lattice *i.e.* octahedrally and tetrahedrally $A1^{3+}$ ions.

While calcination temperature was shown to affect the first desorption step (responsible for H-Py), its effect on the second step (responsible for L-Py) is ineffective. This is in accordance with the thermal analysis and XRD results.

Calcination at higher temperatures leads to a considerable decrease in OH populations (lowering H-Py) and results in a better crystallinity which in turn affects the Lewis sites populations. For AlO-C at 700 °C the crystallinity started to be a dominant factor, where L-Py becomes higher. Increasing the calcination temperature tends to lower these values again as the surface area decreased due to sintering, where the number of available sites are expected to diminish. Fig. 6 shows the temperature programmed desorption of adsorbed pyridine from the 5 %Na_2O and 5 %P_2O_5 modified AlO-C. It is obvious from the figure that modification of AlO-C with Na_2O or P_2O_5 decreases the acidity. Fig. 7, on the other hand, shows that modification with Na_2O has a very little influence on the acidity of the pure AlO-P while P_2O_5 modification increases the acidity to a great extent. The 5 %Na_2O modified AlO-C is amorphous and showed a negligible amount of sodium aluminium oxide, $NaAl_{11}O_{17}$. The 5 % Na_2O modified AlO-P, on the other hand, showed a weak pattern of γ-alumina and a negligible amount of sodium aluminium oxide, $NaAl_5O_8$. The XRD results of the 5 % P_2O_5 modified AlO-C and AlO-P showed amorphous

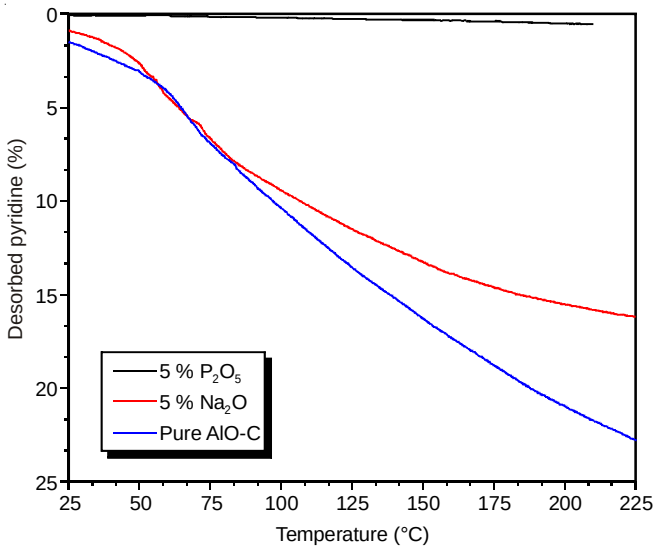

Fig. 6. Temperature programmed desorption (TPD) curves of the adsorbed pyridine over pure and modified AlO-C catalysts calcined at 600 ºC

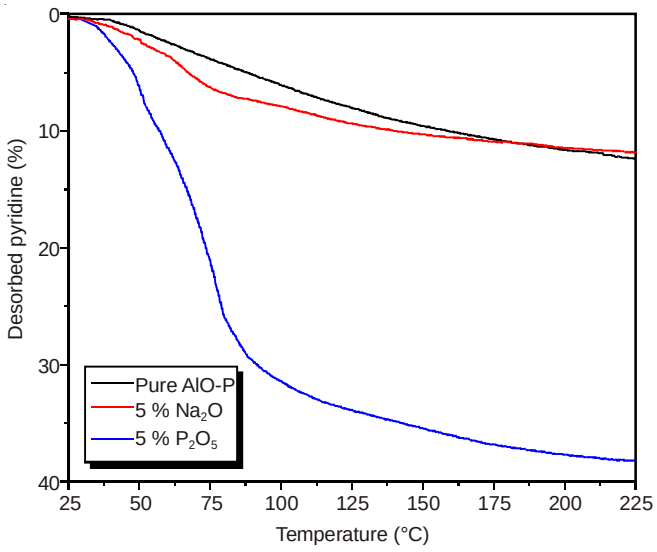

Fig. 7. Temperature programmed desorption (TPD) curves of the adsorbed pyridine over pure and modified AlO-P catalysts calcined at 600 ºC

materials with the formation of a minor proportion of $AlPO_4$ in both cases. There is no appreciable effect as a result of Na_2O modification on the measured acidity of AlO-P. This may indicate that the method of modification of AlO-P, co- precipitation, has resulted in a large decrease in the Brønsted acidity (-OH), while there may be still a large amount of surface Lewis acid sites. This may be through a cation exchange with -OH groups and the formation of Al-ONa groups. The cation exchange of Na^+ with surface OH groups of alumina has been previously studied for potassium modified alumina prepared from K_2CO_3-impregnated alumina[34]. In the present preparation scheme, inclusion of Na^+ in aluminium hydroxide can take place, mainly, by cation exchange process, while inclusion of Na^+ in calcined aluminium nitrate may proceed through this cation exchange or through precipitation in the aluminium bulk during the evaporation process. The increase in acidity due to AlO-P modification with P_2O_5 may be due to the enhancement of both the Brønsted and Lewis acidity.

Pure and modified magnesia: Characterization of magnesia catalysts as well as their parent materials were achieved using the same techniques used for characterization of alumina catalysts, *i.e.* TGA; DTA; XRD and TPD (of formic acid which is used as a probe molecule).

Thermal analysis (TGA and DTA): Table-2 shows the TGA and the DTA data of the two parent materials [*i.e.* $MgCO_3$ and $Mg(OH)_2$] used for the preparation of magnesia catalysts. The TGA of $MgCO_3$ shows two weight loss steps. The first, slow step commences at about 100 °C which was accompanied by 3.9 % weight loss. The second step (between 250-510 °C) is accompanied by 51.6 % weight loss. This brings the total weight loss, after complete decomposition, to 55.51 % of the original weight of sample. Theoretical weight loss calculated for the decomposition of $MgCO_3$ to MgO is 52.18 %. DTA curve shows an endothermic peak maximized at 358 °C.

Magnesium hydroxide on the other hand, decomposes *via* two weight loss steps. The first weight loss step started at 300 °C and extended to 405 °C with a weight loss of 27.1 %. This step is attributed to the decomposition of $Mg(OH)_2$ to MgO. The second weight loss step started at about 500 °C and extended to 525 °C with a weight loss of 1.16 % which is attributed to the dehydroxylation process. This brings the total weight loss to 28.26 % compared to the theoretical weight loss corresponding to the dehydroxylation of $Mg(OH)_2$ to MgO calculated to be 30.87 %. This discrepancy indicates the presence of a reasonable amount of surface –OH groups still present on the magnesia surface up to the calcination temperature of 600 °C. The corresponding DTA curve shows a single endothermic peak attributed to the first weight loss step which is assigned for the decomposition process maximized at 372 °C. The activation energies of the thermal decomposition steps for both magnesia precursors are given in Table-2.

X-ray diffraction analysis: The XRD patterns of magnesia catalysts prepared from magnesium carbonate precursor (denoted as Mg-C) and magnesia catalysts prepared from the hydroxide precursor (denoted as Mg-P) are displayed in Figs. 8 and 9, respectively. Magnesium oxide periclase was the only phase exhibited in both systems. The corresponding peaks intensity was shown to increase with increasing the calcination temperature, for both catalysts systems.

TABLE-2
THERMOGRAVEMTRIC (TGA) AND DIFFERENTIALS THERMOGRAVEMETRIC (DTA) ANALYSIS DATA FOR THE NON-ISOTHERMAL DECOMPOSITION OF $MgCO_3$ AND $Mg(OH)_2$

Sample	TGA data			DTA data T_{max}	ΔE (kJ/mol)
	Decomposition steps	Temperature ranges (°C)	Mass loss (%)		
$MgCO_3$	1	30-100	3.90	–	60.0
	2	250-510	51.60	358 ºC	
$Mg(OH)_2$	1	300-405	27.10	372 ºC	143.0
	2	500-530	1.16		

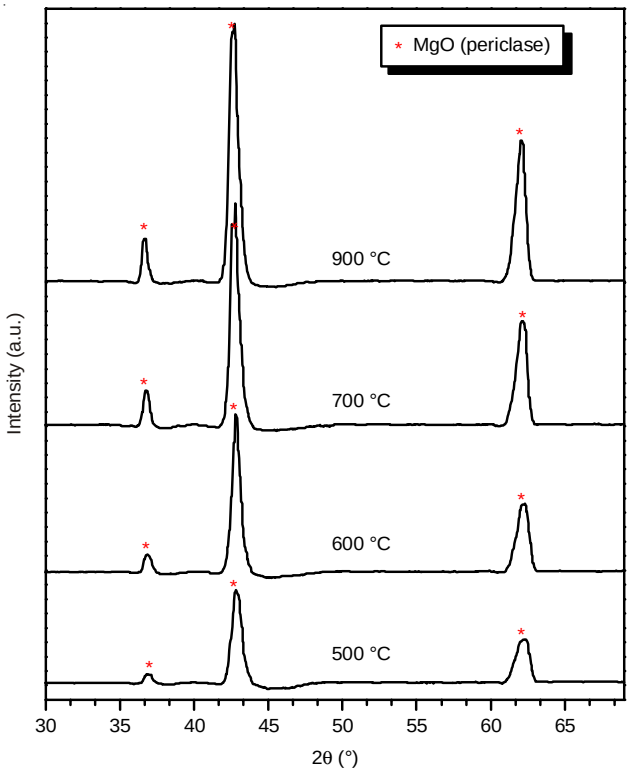

Fig. 8. XRD patterns of Mg-C catalysts calcined at different temperatures

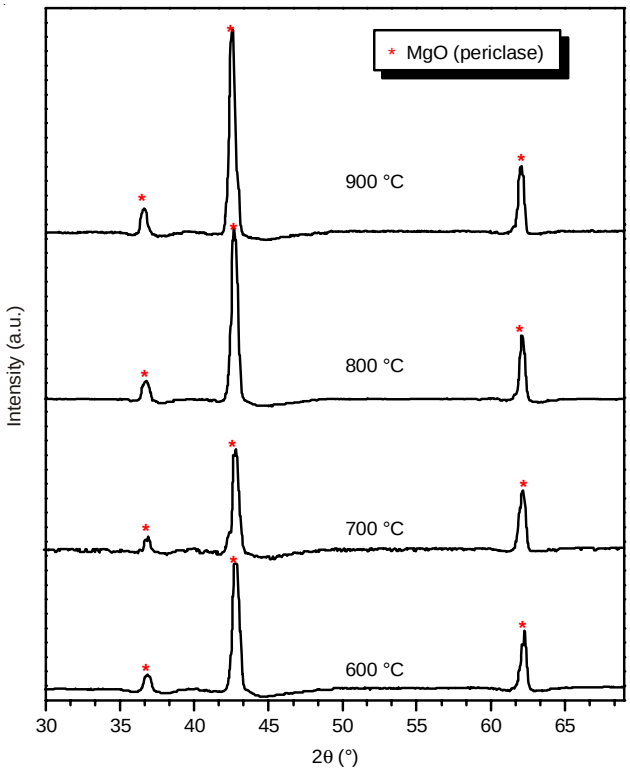

Fig. 9. XRD patterns of Mg-P catalysts calcined at different temperatures

Basicity measurements (temperature programmed desorption): Magnesia (which is one of the alkaline earth oxides) shows a surface basicity. Surface acidity was also observed on magnesia surface where centres of different acidity are formed on the surface of MgO calcined in air up to 600 °C. The basic strength decreased and acidic strength increased as the heating temperature of magnesia increased[34]. The Brønsted acidity on magnesia surface may be due to the presence of the hydroxyl groups. The basic sites are strongly basic O^{2-} centres adjacent to the surface OH groups and surface OH groups which constitute weak basic sites.

Figs. 10 and 11 show the temperature programmed desorption (TPD) of the adsorbed formic acid on the surface of Mg-C and Mg-P catalysts, respectively. It is obvious that the basicity reaches its maximum for samples calcined at 600 °C then decreases for samples calcined at 700 °C for both systems. The basicity of Mg-C and Mg-P systems begins to increase again for the samples calcined at 800 and 900 °C in both systems. The maximum value of the measured basicity for Mg-C and Mg-P systems is obtained by calcining the starting materials $MgCO_3$ and $Mg(OH)_2$ at 600 and 900 °C, respectively. The basicity minima observed for both catalyst samples calcined at 700 °C may be due to the intensive dehydroxylation following the increase in the calcination temperature. The increase in basicity observed for samples calcined at higher temperatures (> 700 °C) may be due to the appearance of another type of basic sites. These sites are called the reducing sites[1].

From the above presented results, the following points could be concluded:

• Mg-C samples, always, exhibit higher basicity than the corresponding samples of Mg-P as represented in Fig. 12.

• Desorption of formic acid occurred through two different and interfered, desorption steps. This may reflect the heterogeneity of the surface basic sites.

• The sample calcined at 600 °C of Mg-C system and that calcined at 900 °C of Mg-P system showed the highest basicity in the two systems.

The basicity of magnesia can be changed as a result of doping with guest ions. The effect of modification of magnesia catalysts with basic oxides (*e.g.* Na_2O) or acidic oxides (*e.g.* P_2O_5) on its basicity was studied. It was previously shown[27] that modification of magnesia with a suitable amounts of K^+, Al^{3+} or Zr^{4+} increases both the concentration and the strength of basic sites.

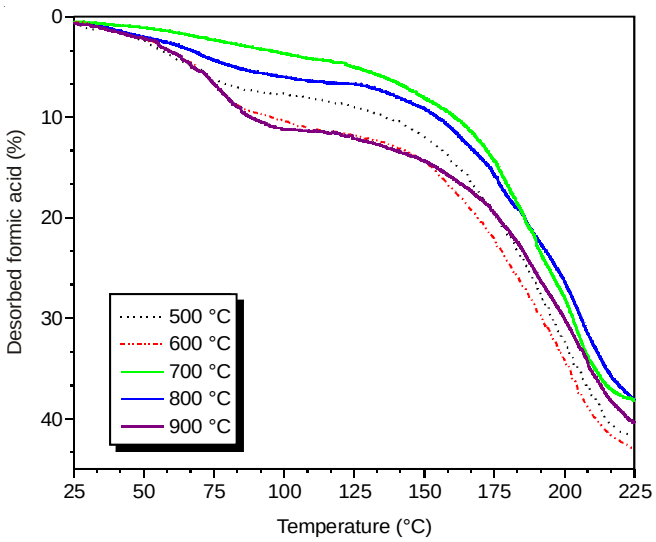

Fig. 10. Temperature programmed desorption (TPD) curves of the adsorbed formic acid over Mg-C catalysts calcined at different temperatures

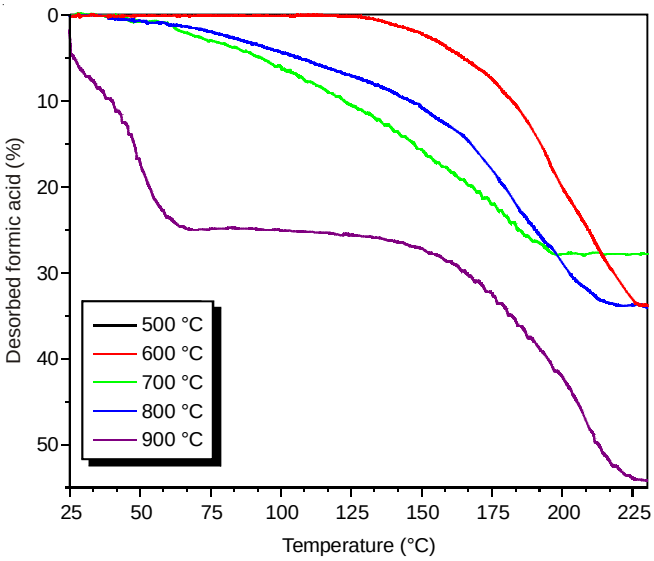

Fig. 11. Temperature programmed desorption (TPD) curves of the adsorbed formic acid over Mg-P catalysts calcined at different temperatures

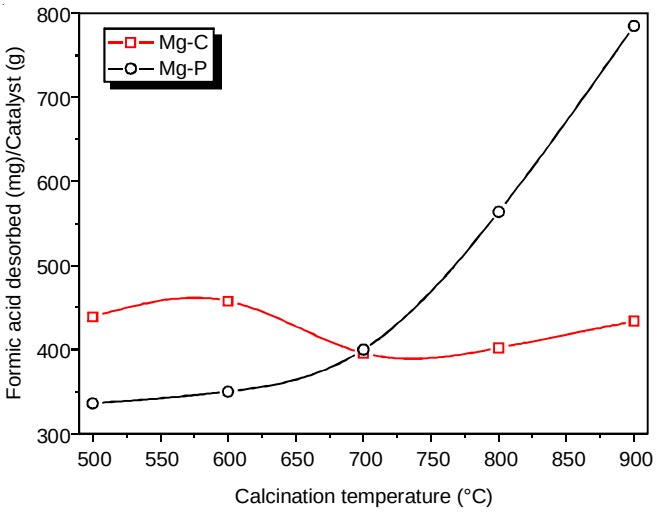

Fig. 12. Acidity of pure magnesia catalysts (C and P) calcined at different temperatures

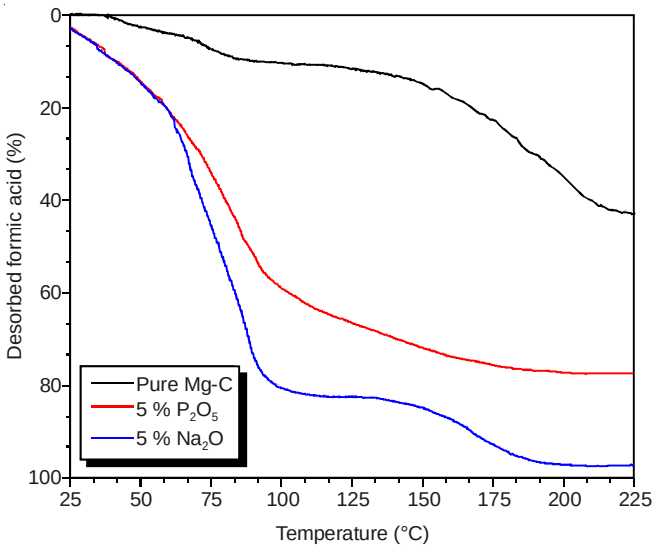

Fig. 13. Temperature programmed desorption (TPD) curves of the adsorbed formic acid over pure and modified Mg-C catalysts calcined at 600 ºC

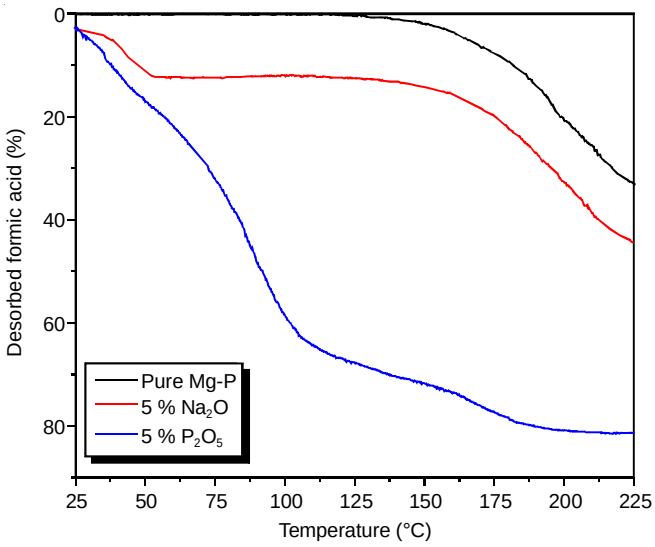

Fig. 14. Temperature programmed desorption (TPD) curves of the adsorbed formic acid over pure and modified Mg-P catalysts calcined at 600 ºC

The temperature programmed desorption of adsorbed formic acid on modified magnesia Mg-C is displayed in Fig. 13. It is evident that the basicity increased largely due to Na_2O and P_2O_5 modification. On the other hand, Fig. 14 shows the temperature programmed desorption of formic acid on modified magnesia Mg-P surface. It shows that modification of MgO with 5 % Na_2O has resulted in a considerable increase in basicity, while, a larger increase in basicity was observed for the 5 % P_2O_5 modified sample. The XRD results of P_2O_5 modified Mg-C has shown the formation of farrigtonite and $Mg_3(PO_4)_2$ magnesium phosphate besides the major MgO periclase. $Mg_2P_2O_7$ was also detected besides the MgO periclase for the P_2O_5 modified Mg-P. No other products were observed with the MgO periclase for the Na_2O modified samples.

Conclusion

The acidic and basic centres on the surface of metal oxides catalysts are known to influence their catalytic activity. The variation of acidity (or basicity) of catalysts by a number of variables was carried out by the adsorption of basic or acidic vapour molecules. For example, alumina showed strong surface acidity of both types, Brønsted and Lewis. The calcination temperature of alumina does influence its acidic properties where Al_2O_3 shows two acidity maxima at 500 °C and between 700-800 °C with acidity minima at 600 °C. Al_2O_3 was shown, also, to possess some basic sites. MgO, on the other hand, is shown to possess several types of basic centres.

REFERENCES

1. B.C. Gates, Catalytic Chemistry, John Wiley & Sons, New York (1992).
2. J.F. Le Page, J. Cosyns, P. Courty, E. Freund, J.P. Franck, Y. Jacquin, B. Juguin, C. Marcilly, G. Martino, J. Miquel, R. Montamal, A. Sugier and H. Van Landeghem, Applied Heterogeneous Catalysis, Editions Techip, Paris (1987).
3. A.B. Stiles, Catalyst Supports and Supported Catalysts, Butterworth, London (1987).

4. L.D. Hart, Alumina Chemicals, The American Ceramic Society, Westerville, Ohio (1990).
5. L. Damjanovic and A. Auroux, Handbook of Thermal Analysis and Calorimetry, vol. 5, Ch. 11, p. 387 (2008).
6. A.B. Sherrill and M.A. Barteau, *Chem. Phys. Solid Surf.*, **9**, 409 (2001).
7. T. Seki and M. Onaka, *J. Mol. Catal. Chem.*, **263**, 115 (2007).
8. G. Busca, T. Montanari, M. Bevilacqua and E. Finocchio, *Colloids Surf. A*, **320**, 205 (2008).
9. E. Rombi, M.G. Cutrufello, S. De Rossi, M.F. Sini and I. Ferino, *J. Mol. Catal. Chem.*, **247**, 171 (2006).
10. L. Liu, J. Cai, L. Qi, Q. Yu, K. Sun, B. Liu, F. Gao, L. Dong and Y. Chen, *J. Mol. Catal. Chem.*, **327**, 1 (2010).
11. D. Liu, C. Yao, J. Zhang, D. Fang and D. Chen, *Fuel*, **90**, 1738 (2011).
12. Y. Fu, T. Hong, J. Chen, A. Auroux and J. Shen, *Thermochim. Acta*, **434**, 22 (2005).
13. S.H.C. Liang and I.D. Gay, *J. Catal.*, **101**, 293 (1986).
14. R.S. Araújo, D A S. Maia, D.C.S. Azevedo, C.L. Cavalcante Jr., E. Rodríguez-Castellón and A. Jimenez-Lopez, *Appl. Surf. Sci.*, **255**, 6205 (2009).
15. A. Gervasini, P. Carniti and A. Auroux, *Thermochim. Acta*, **434**, 42 (2005).
16. S.B. Gürel and A. Altun, *Powder Technol.*, **196**, 115 (2009).
17. J. Kirchnerova, D. Klvana and J. Chaouki, *Appl. Catal. A*, **196**, 191 (2000).
18. M. Simionato and E.M. Assaf, *Mater. Res.*, **6**, 535 (2003).
19. I. Tankov, B. Pawelec, K. Arishtirova and S. Damyanova, *Appl. Surf. Sci.*, **258**, 278 (2011).
20. A.M. Youssef and Th. El-Nabarawy, *J. Serb. Chem. Soc*., **53**, 377 (1988).
21. A. Corma and S. Iborra, *Adv. Catal.*, **49**, 239 (2006).
22. C. Pighini, T. Belin, J. Mijoin, P. Magnoux, G. Costentin and H. Lauron-Pernot, *Appl. Surf. Sci.*, **257**, 6952 (2011).
23. Y. Xi and R.J. Davis, *J. Mol. Catal. Chem.*, **341**, 22 (2011).
24. M. Mollavali, F. Yaripour, Sh. Mohammadi-Jam and H. Atashi, *Fuel Process. Technol.*, **90**, 1093 (2009).
25. K. Sugiyama, Y. Nakano, H. Souri, E. Konuma and T. Matsuda, *J. Mater. Chem.*, **4**, 1897 (1994).
26. G. Zhang, T. Tanaka, T. Yamaguchi, H. Hattori and K. Tanabe, *J. Phys. Chem.*, **94**, 506 (1990).
27. M.A. Aramendía, V. Borau, C. Jiménez, A. Marinas, J.M. Marinas, J.R. Ruiz and F.J. Urbano, *J. Mol. Catal. A*, **218**, 81 (2004).
28. F. Aberuagba, M. Kumar, J.K. Gupta, G. Muralidhar and L.D. Sharma, *Reac. Kine. Catal. Lett.*, **75**, 245 (2002).
29. H. Kawakami and S. Yoshida, *J. Chem. Soc., Faraday Trans. II*, **80**, 921 (1984).
30. T. Iizuka, H. Hattori, Y. Ohno, J. Sohma and K. Tanabe, *J. Catal.*, **22**, 130 (1971).
31. H. Hattori, N. Yoshii and K. Tanabe, in ed.: J.W. Hightower, Proc. 5th Int. Congr. Catal., Miami Beach, 1972, Pub. North Holland, Amsterdam, p. 233 (1973).
32. JCPDS-International Centre for Diffraction Data, CD (1996).
33. J.W. Coats and J.P. Redfern, *Nature*, **201**, 68 (1964).
34. M.C. Wu and D.W. Goodman, *Catal. Lett.*, **15**, l (1992).